Application of the finite-temperature Lanczos method for the evaluation of magnetocaloric properties of large magnetic molecules

Jürgen Schnack and Christian Heesing

Department of Physics, Bielefeld University, P.O. box 100131, D-33501 Bielefeld, Germany

Abstract. We discuss the magnetocaloric properties of gadolinium containing magnetic molecules which potentially could be used for sub-Kelvin cooling. We show that a degeneracy of a singlet ground state could be advantageous in order to support adiabatic processes to low temperatures and simultaneously minimize disturbing dipolar interactions. Since the Hilbert spaces of such spin systems assume very large dimensions we evaluate the necessary thermodynamic observables by means of the Finite-Temperature Lanczos Method.

1 Introduction

The use of magnetic molecules for sub-Kelvin cooling is one of the latter ideas in the field of molecular magnetism. Originally paramagnetic salts have been employed for this purpose which in 1949 led to the Nobel prize for William Francis Giauque [1]. In recent years several molecular systems have been discussed with respect to their magnetocaloric properties [2,3,4,5,6,7,8]. Some aspects have turned out to be of importance if one wants to compete with the cooling power of paramagnetic salts: the low-lying energy eigenstates should possess large magnetic moments and they should be dense, so that one can sweep many of them with moderate magnetic fields. The magnetic anisotropy should be small, otherwise energy barriers could prevent a high density of states. These aspects make gadolinium the preferred metal ion: it has a large spin quantum number of $s = 7/2$, a rather small exchange interaction in chemical complexes and a negligible single-ion anisotropy, compare e.g. Refs. [5,6,7].

From the point of view of theoretical modeling gadolinium compounds are demanding since the sizes of the respective Hilbert spaces grow very rapidly with the number of involved gadolinium ions due to the large spin quantum number. Even when employing all possible symmetries the system size is rather restricted since the dimension of the largest subspace should not exceed a size of 100,000 in order to render a complete numerical diagonalization possible [9,10]. Fortunately, a very accurate approximation has been developed for cases with Hilbert space dimensions of up to roughly 10^{10} – the Finite Temperature Lanc-

zos Method (FTLM) [11,12]. In a recent publication we demonstrated that this method is indeed capable of evaluating thermodynamic observables for magnetic molecules with an accuracy that is nearly indistinguishable from exact results [13].

The interesting physical question is, which arrangements of interacting magnetic ions permit a large magnetocaloric effect. For this purpose the low-lying zero-field density of states should be high, and an applied field should fan out these levels. Magnetic frustration is known to yield dense spectra and to enhance the magnetocaloric effect under certain circumstances [14,15,16]. In addition frustration, i.e. a situation where not all pairs of spins assume a collinear arrangement in the classical ground state [17], may result in singlet ground states which are degenerate. This would have two advantageous consequences: the ground state would be connected to an isentrope with $S > 0$ which should allow for very low-temperature cooling. In addition a singlet ground state minimizes the dipolar interactions compared to high-spin molecules where dipolar interactions prevent a cooling to very low-temperatures [18]. We investigate our hypothesis with the simplest of such systems, the tetrahedron.

It should be mentioned that one can also aim at designing the intermolecular interactions in order to reduce the influence of dipolar interactions [18]. The most simple way consists in increasing the mutual distances by means of bulky ligands. This route will not be discussed in the present article.

The article is organized as follows. In Section 2 basics of the finite-temperature Lanczos method are repeated. Section 3 is devoted to the discussion of several recently

synthesized gadolinium containing compounds. The article closes with a summary. A technical appendix explains a basis coding scheme used in the FTLM.

2 The finite-temperature Lanczos method

For the evaluation of thermodynamic properties in the canonical ensemble the exact partition function Z depending on temperature T and magnetic field B is given by

$$Z(T,B) = \sum_{\nu} \langle \nu | e^{-\beta \underset{\sim}{H}} | \nu \rangle \; . \qquad (1)$$

Here $\{| \nu \rangle\}$ denotes an orthonormal basis of the respective Hilbert space. Following the ideas of Refs. [11,12] the unknown matrix elements are approximated as

$$\langle \nu | e^{-\beta \underset{\sim}{H}} | \nu \rangle \approx \sum_{n=1}^{N_L} \langle \nu | n(\nu) \rangle e^{-\beta \epsilon_n^{(\nu)}} \langle n(\nu) | \nu \rangle \; . \quad (2)$$

For the evaluation of the right hand side of Eq. (2) $| \nu \rangle$ is taken as the initial vector of a Lanczos iteration. This iteration consists of N_L Lanczos steps, which span a respective Krylow space. As common for the Lanczos method the Hamiltonian is diagonalized in this Krylow space. This yields the N_L Lanczos eigenvectors $| n(\nu) \rangle$ as well as the associated Lanczos energy eigenvalues $\epsilon_n^{(\nu)}$. They are enumerated by $n = 1, \ldots, N_L$. The notation $n(\nu)$ is chosen to remind one that the Lanczos eigenvectors $| n(\nu) \rangle$ belong to the Krylow space derived from the original state $| \nu \rangle$.

The number of Lanczos steps N_L is a parameter of the approximation that needs to be large enough to reach the extremal energy eigenvalues but should not be too large in order not to run into problems of numerical accuracy. $N_L \approx 100$ is a typical and good value.

In addition, the complete and thus very large sum over all states $| \nu \rangle$ is replaced by a summation over a subset of R random vectors. These vectors are truly random, they do not need to belong to any special basis set. Altogether this yields for the partition function

$$Z(T,B) \approx \frac{\dim(\mathcal{H})}{R} \sum_{\nu=1}^{R} \sum_{n=1}^{N_L} e^{-\beta \epsilon_n^{(\nu)}} |\langle n(\nu) | \nu \rangle|^2 \; . \quad (3)$$

It will of courseimprove the accuracy if symmetries are taken into account as in the following formulation

$$Z(T,B) \approx \sum_{\Gamma} \frac{\dim(\mathcal{H}(\Gamma))}{R_\Gamma} \sum_{\nu=1}^{R_\Gamma} \sum_{n=1}^{N_L}$$
$$\times e^{-\beta \epsilon_n^{(\nu,\Gamma)}} |\langle n(\nu,\Gamma) | \nu,\Gamma \rangle|^2 \; . \qquad (4)$$

Γ labels the irreducible representations of the employed symmetry group. The complete Hilbert space is decomposed into mutually orthogonal subspaces $\mathcal{H}(\Gamma)$.

An observable would then be calculated as

$$O(T,B) \approx \frac{1}{Z(T,B)} \sum_{\Gamma} \frac{\dim(\mathcal{H}(\Gamma))}{R_\Gamma} \sum_{\nu=1}^{R_\Gamma} \sum_{n=1}^{N_L} e^{-\beta \epsilon_n^{(\nu,\Gamma)}}$$
$$\times \langle n(\nu,\Gamma) | \underset{\sim}{Q} | \nu,\Gamma \rangle \langle \nu,\Gamma | n(\nu,\Gamma) \rangle \; . \quad (5)$$

This approximation of the observable $O(T,B)$ may contain large statistical fluctuations at low temperatures due to the randomness of the set of states $\{| \nu, \Gamma \rangle\}$, but this can be cured by assuming a symmetrized version of Eq. (5) [19]. For our investigations this is irrelevant.

In this article the entropy plays a central role, it is evaluated as

$$S(T,B) = \langle\langle \underset{\sim}{H} \rangle\rangle / T + k_B \log(Z(T,B)) \; , \qquad (6)$$

with $Z(T,B)$ being calculated according to (4) and $\langle\langle \underset{\sim}{H} \rangle\rangle$ according to (5).

Our very positive experience is that even for large problems the number of random starting vectors as well as the number of Lanczos steps can be chosen rather small, e.g. $R \approx 20, N_L \approx 100$, compare Ref. [13].

3 Magnetocalorics of certain gadolinium compounds

The following spin systems are described by the Heisenberg spin Hamiltonian augmented with a Zeeman term, i.e.

$$\underset{\sim}{H} = -2 \sum_{i<j} J_{ij} \underset{\sim}{s}_i \cdot \underset{\sim}{s}_j + g\,\mu_B\,B \sum_i \underset{\sim}{s}_i^z \; . \qquad (7)$$

J_{ij} is the exchange parameter between spins at sites i and j. For the sake of simplicity it is assumed that all spins have the same g-factor. Since $\left[\underset{\sim}{H}, \underset{\sim}{S}^z\right] = 0$, this (simple) symmetry is used for the finite-temperature Lanczos calculations.

In a process of adiabatic demagnetization the temperature changes with field according to the following thermodynamic relation:

$$\left(\frac{\partial T}{\partial B}\right)_S = -\frac{T}{C} \left(\frac{\partial S}{\partial B}\right)_T \; . \qquad (8)$$

Here S denotes entropy, T temperature, B magnetic induction, and C heat capacity. Besides the heat capacity, which in our examples does not vary too much for small fields and temperatures $T \approx 1$ K, the isothermal entropy change $\left(\frac{\partial S}{\partial B}\right)_T$ has a large impact [8]. At very low temperatures close to $T = 0$ the isothermal entropy change is of course very large if the ground state of the magnetic molecule possesses a large total spin quantum number S_t, since this corresponds to a theoretical entropy of $S(T = 0, B = 0) = k_B \log(2S_t + 1)$.[1] Therefore, naively

---

[1] Here a short remark concerning the third law of thermodynamics might be necessary: The third law conjectures that at $T = 0$ the entropy of any system is a universal constant that can be taken to be $S = 0$ which in turn means that the ground state is non-degenerate. Models, however, can show a ground state degeneracy and thus a residual entropy at $T = 0$. In reality tiny interactions might split this degeneracy at their energy scale, which means that the residual entropy remains at its value down to this scale.

thinking, all isentropes with an entropy equal to or smaller than this value should run into absolute zero. How close they come in reality depends on the very small interactions that become relevant at very low temperatures. The most disturbing interaction for high-spin molecules is the dipolar interaction, which also in the case of paramagnetic salts limits the achievable temperatures. In the following we therefore also discuss a possible way out of this dilemma: molecules that possess an $S_t = 0$ ground state with residual entropy due to a ground state degeneracy.

3.1 Gd$_4$Cu$_8$ & Gd$_4$Ni$_8$

The M=Cu and M=Ni members of the family of Gd$_4$M$_8$ molecules were synthesized quite recently [7]. The eigenvalues of the respective spin Hamiltonians could be determined numerically exactly for the case of Gd$_4$Cu$_8$, but not for Gd$_4$Ni$_8$. In the latter case the Finite-Temperature Lanczos Method was employed.

For Gd$_4$Cu$_8$ the model Hamiltonian (7) includes the following parameters: $J_{GdGd} = -0.1$ cm^{-1}, $J_{GdCu} = +0.9$ cm^{-1}, $J_{CuCu} = -8.0$ cm^{-1}. The spectroscopic splitting factor was taken as $g = 2.0$. For Gd$_4$Ni$_8$ the model parameters were chosen as: $J_{GdGd} = -0.1$ cm^{-1}, $J_{GdNi} = +0.17$ cm^{-1}, $J_{NiNi} = +12.0$ cm^{-1}. Again we took $g = 2.0$. In the following all other interactions or corrections such as temperature independent paramagnetism, different g factors for different ions or a possible single-ion anisotropy in the case of nickel have been neglected. Despite these approximations all theoretical curves agree nicely with the experimental ones published in Ref. [7].
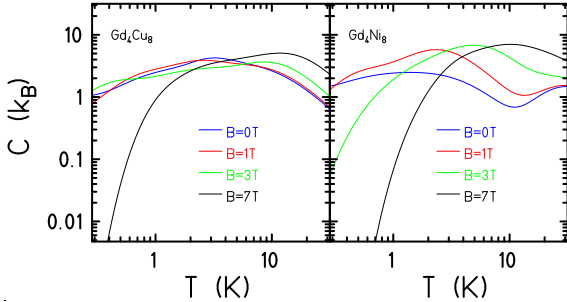

Fig. 1. Theoretical heat capacity per molecule for Gd$_4$Cu$_8$ (l.h.s.) and Gd$_4$Ni$_8$ (r.h.s.) at various magnetic fields.

Figure 1 displays the theoretical heat capacity per molecule for Gd$_4$Cu$_8$ (l.h.s.) and Gd$_4$Ni$_8$ (r.h.s.) at various magnetic fields. The behavior is for both compounds qualitatively similar.

The isothermal magnetic entropy change, compare Fig. 2, turns out to be very different; it is much larger for Gd$_4$Ni$_8$. The reason is that for Gd$_4$Ni$_8$ the low-lying multiplets belong to large total spin quantum numbers which leads to larger entropies at low temperatures. This is made even clearer in the two following plots displaying the isentropes as function of both temperature and magnetic field.
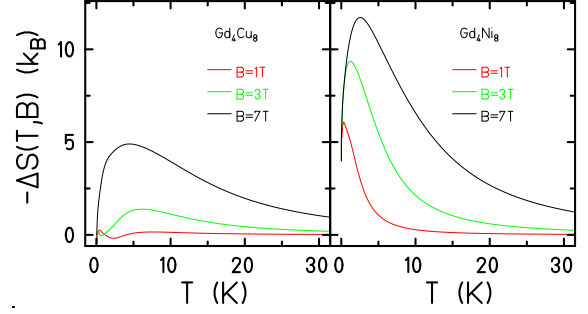
Fig. 2. Theoretical isothermal entropy change per molecule for Gd$_4$Cu$_8$ (l.h.s.) and Gd$_4$Ni$_8$ (r.h.s.) for various field differences: $-\Delta S(T, B) = -[S(T, B) - S(T, 0)]$.
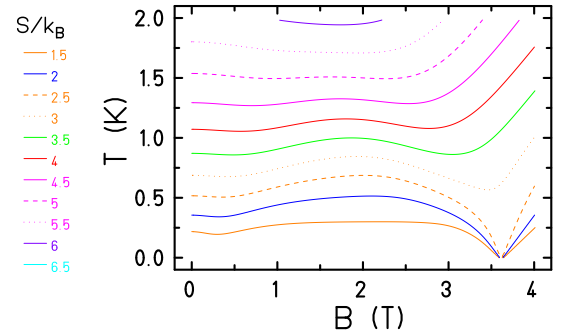
Fig. 3. Theoretical isentropes for Gd$_4$Cu$_8$.
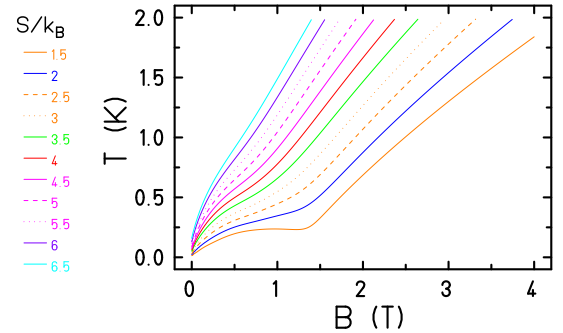
**Fig. 4.** Theoretical isentropes for Gd$_4$Ni$_8$.

Gd$_4$Cu$_8$ (Fig. 3) possesses a non-degenerate $S_t = 0$ ground state that is separated from a triplet and a quintet, whereas Gd$_4$Ni$_8$ (Fig. 4) has a ground state with $S_t = 22$. In the latter case all isentropes with $S \leq k_B \log(45)$ run into absolute zero, which is clearly visible in Fig. 4. On the contrary, since Gd$_4$Cu$_8$ possesses a non-degenerate $S_t = 0$ ground state all isentropes approach temperatures $T > 0$ when B goes to zero.

Although this behavior suggests that Gd$_4$Ni$_8$ should be a very good refrigerant, this does not need to be the case. At sub-Kelvin temperatures dipolar interactions become very important. They prevent a closer approach of $T = 0$ [18]. Dipolar interactions could be tamed by molecules that possess an $S_t = 0$ ground state, but a non-degenerate ground state would not be helpful due to its vanishing entropy. Therefore, we suggest to investigate molecules which have a degenerate – the more the better – ground

state with $S_t = 0$. A ground state degeneracy can be induced by frustration, thus a tetrahedron with antiferromagnetic coupling would be a first candidate.

3.2 A fictitious Gd$_4$ tetrahedron

About half a dozen Gd$_4$ tetrahedra have been synthesized to date, none of them was magnetically characterized [20, 21, 22, 23, 24, 25]. In the following we therefore discuss the magnetic properties of a fictitious Gd$_4$ tetrahedron with an exchange interaction of $J_{\mathrm{GdGd}} = -0.1$ cm^{-1} and $g = 2.0$. The magnetic heat capacity (not shown) looks pretty similar to those already shown; again $C \approx 1 k_B$ for low fields at $T \approx 1$ K.
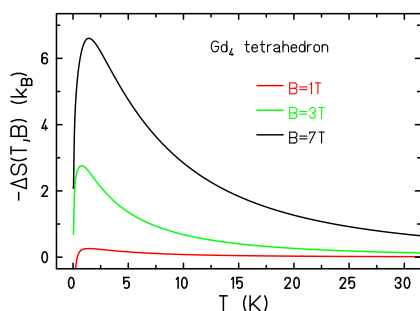
Fig. 5. Theoretical isothermal entropy change per molecule for a Gd$_4$ tetrahedron for various field differences.

The isothermal magnetic entropy change, compare Fig. 5, looks unspectacular. Nevertheless, the isentropes shown in Fig. 8 demonstrate an unusual behavior which is not obvious at first glance. Since the $S = 0$ ground state is eightfold degenerate all isentropes with $S \leq k_B \log(8) = 2.08 k_B$ run into absolute zero. But for a tetrahedron this happens in a different way compared to molecules with high-spin ground state such as Gd$_4$Ni$_8$. The isentropes of high-spin molecules approach zero like a paramagnet with a rate of

$$\left(\frac{\partial T}{\partial B} \right)_S \approx \frac{T}{B} \; , \qquad (9)$$

i.e. rather steeply. For molecules with a diamagnetic ground state zero is approached on a rather "flat" trajectory, e.g. from high magnetic fields values like $B = 4$ T at $T = 1$ K, compare Fig. 6.

Figure 7 shows the related magnetization contour plot. While decreasing the magnetic field also the magnetization decreases and consequently also the dipolar interaction.

3.3 A Gd$_6$ octahedron

As a last example we would like to discuss the octahedron. This is another interesting structure since it is not too complicated to be synthesized and it has an interesting spectrum. The spectrum of an octahedron is that of a
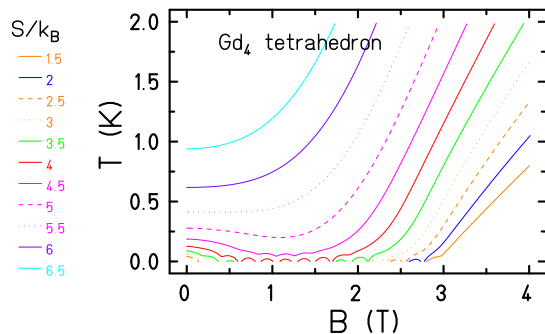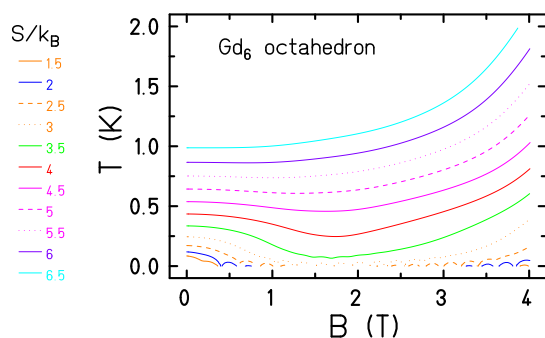

Fig. 6. Theoretical isentropes for a Gd$_4$ tetrahedron. The lowest isentropes overlap at $T = 0$ in this linear plot.
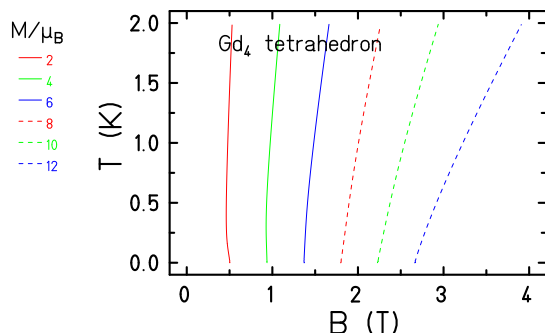
**Fig. 7.** Theoretical magnetization contours for a Gd$_4$ tetrahedron.

so-called three-sublattice antiferromagnet [26]. The non-degenerate ground state possesses $S_t = 0$, higher-lying multiplets are highly degenerate beyond their usual degeneracy due to magnetic sublevels. The weak point nevertheless is the non-degenerate ground state which precludes successful cooling, compare isentropes in Fig. 8.


Fig. 8. Theoretical isentropes for a Gd$_6$ octahedron. The lowest isentropes overlap at $T = 0$ in this linear plot.

In addition to the perfect octahedron we would like to discuss a recently synthesized distorted octahedron [27]. We assume that this octahedron has an approximate C_4 symmetry. Four spins are arranged on the vertices of a square, one at the top, another one at the bottom. A rough simulation of the available experimental data yielded the following exchange integrals: the interaction between top

(or bottom) and every spin of the square $J_{\text{ts}} = J_{\text{bs}} = -0.05$ cm^{-1}, between nearest neighbors on the square $J_{\text{ss}} = -0.02$ cm^{-1}, and between top and bottom spins $J_{\text{tb}} = -0.2$ cm^{-1}. The spectroscopic splitting factor was taken as $g = 2.0$.
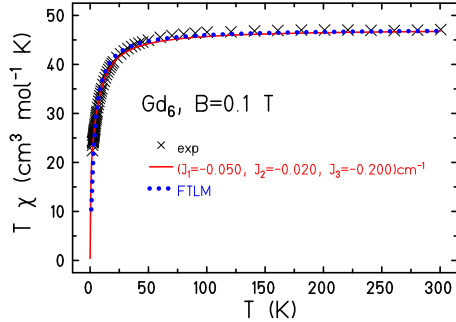

Fig. 9. Experimental and theoretical susceptibility of the distorted octahedron. Experimental values taken from Ref. [27]. The solid curve is the result of a complete diagonalization, the dots result from the FTLM.
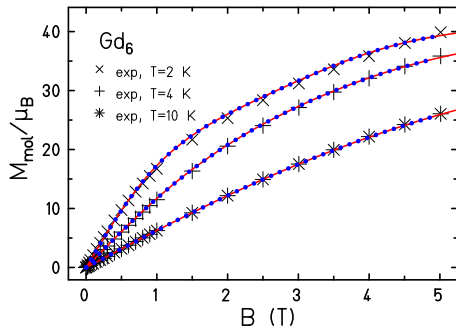
Fig. 10. Experimental and theoretical magnetization of the distorted octahedron. Experimental values taken from Ref. [27]. The solid curve is the result of a complete diagonalization, the dots result from the FTLM.

As one can see in Figs. 9 and 10 a coupling scheme with the above given exchange interactions yields a very good approximation of the experimental data. We can now predict how this material would behave as an adiabatic cooler. Figure 11 depicts the isentropes of the distorted octahedron.

Although also this molecule has a non-degenerate diamagnetic ground state the isentropes exhibit a much steeper slope, i.e. larger cooling rate, compared to the regular octahedron. We conjecture that this results from the fact that the non-symmetric, i.e. only C_4 symmetric interactions split the highly degenerate multiplets and thus lead to a smeared out density of states. In addition, some of the interactions are smaller than in the example or a regular octahedron which also reduces the size of low-lying gaps.
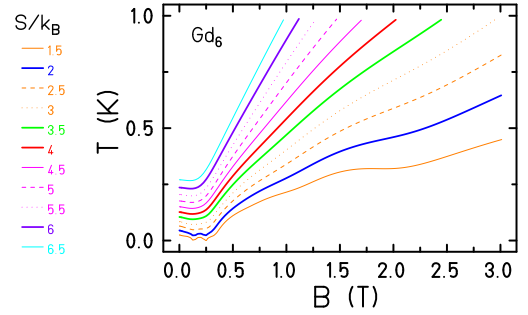
Fig. 11. Theoretical isentropes for the distorted Gd$_6$ octahedron.

4 Summary and Outlook

The Finite-Temperature Lanczos Method enabled us to evaluate the thermal properties of larger gadolinium containing magnetic molecules. Due to the large intrinsic spin of gadolinium these substances are potentially useful sub-Kelvin coolers. A major quality criterion is the achievable ground state degeneracy. If such a degeneracy could be realized for a singlet ground state this would also minimize disturbing dipolar interactions.

Acknowledgment

A Basis coding for mixed spin systems

Since Lanczos iterations consist of matrix vector multiplications they can be parallelized by `openMP` directives [28]. In our programs this is further accelerated by an analytical state coding and an evaluation of matrix elements of the Heisenberg Hamiltonian "on the fly".

To this end an analytical coding for the product basis states

$$| m_1, \ldots, m_u, \ldots, m_N \rangle \tag{10}$$

is needed. Such a coding was already devised in Ref. [28] for equal spins. Here we show that this scheme can be easily generalized for spin systems consisting of different spins s_i, so that $-s_i \leq m_i \leq s_i$. For encoding purposes,

and since m_u can be half-integer, the basis states are usually rewritten in terms of quantum numbers $a_i = s_i - m_i$ instead of m_i, where $a_i = 0, 1, \ldots, 2s_i$.

The non-trivial technical problem of the coding stems from the fact that one wants to use the $\underset{\sim}{S^z}$ symmetry, i.e. work in subspaces $\mathcal{H}(M)$ of total magnetic quantum number M. M assumes values from $-M_{\text{Max}}$ up to M_{Max} with $M_{\text{Max}} = \sum_i s_i$. The basis in the subspace $\mathcal{H}(M)$ is given by all product states $|a_1, \ldots, a_N\rangle$ with $M = M_{\text{Max}} - \sum_i a_i$. For usage in a computer program they need to be assigned to integer numbers $1, \ldots, \dim(\mathcal{H}(M))$. The reason is that one usually does not need the basis only once at initialization, but at every Lanczos iteration, since the sparse Hamiltonian matrix is not stored, but its non-zero matrix elements are evaluated whenever needed using

$$\langle i \, | \, \underset{\sim}{H} \, | \, j \rangle \equiv \langle a_1^i, \ldots, a_N^i \, | \, \underset{\sim}{H} \, | \, a_1^j, \ldots, a_N^j \rangle \, . \quad (11)$$

For a direct coding algorithm of basis states in subspaces $\mathcal{H}(M)$ it is advantageous that the sizes of the subspaces $\mathcal{H}(M)$ are known analytically [29]. Thus an array can be built at startup that contains for a fixed sequence $s_1, s_2, \ldots, s_N$ the sizes of these subspaces $\mathcal{H}(M = M_{\text{Max}} - A)$ for given a given number n of spins and A. We will call this array $D(N, A)$. It will be used to determine the sequential number of a basis vector in $\mathcal{H}(M)$. The recursive buildup is performed using the following relation between the sizes of subspaces

$$D(n, A) = \sum_{k=0}^{2s_n} D(n-1, A-k) \, . \quad (12)$$

If $A \notin \{0, 1, \ldots, 2M_{\text{Max}}\}$ then $D(n, A) = 0$.
For $D(n = 1, A = 0, 1, \ldots, 2s_n) = 1$, $D(n, A = 0) = 1$, and $D(n, A = 1) = n$. If $A \notin \{0, 1, \ldots, 2M_{\text{Max}}\}$ then $D(n, A) = 0$.

A.1 $i \Rightarrow |a_1^i, \ldots, a_N^i\rangle$

One coding direction, $i \Rightarrow |a_1^i, \ldots, a_N^i\rangle$, which is the more trivial direction, can be realized in several ways. A direct algorithm $i \Rightarrow |a_1^i, \ldots, a_N^i\rangle$ using the known dimensions of the subspaces $\mathcal{H}(M = Ns - A)$ could be realized as follows[2]

```
      m=0
      Ak = A
      do k=N,2,-1
         do n=0,2*s(k)
   if(i.le.(m+D(k-1,Ak-n+1))) then
      BasisVector(k) = n
      Ak = Ak - n
      goto 100
```

---

² The given code uses FORTRAN notation. Nevertheless, it can be easily transformed into C. One should only pay attention to the fact that field indices in FORTRAN start at 1 not at 0. Therefore, the definition of the second field index of D has been modified accordingly.

```
      else
   m = m + D(k-1,Ak-n+1)
      endif
      enddo
100   continue
   enddo
   BasisVector(1) = Ak
```

`BasisVector` contains the N entries a_k. This algorithm will be made clearer when we explain the inverse algorithm below.

A.2 $|a_1^i, \ldots, a_N^i\rangle \Rightarrow i$

The inverse direction is actually the nontrivial one, since the basis vectors are only a subset of the full basis set (10). Therefore, for the latter coding direction search algorithms are often employed,[30] or the two-dimensional representation of Lin is used [31].

The position of a basis vector $|a_1, \ldots, a_N\rangle$ in the lexicographically ordered list of vectors will be determined by evaluating how many vectors lay before this vector. For this purpose the known dimensions of the subspaces $\mathcal{H}(M = M_{\text{Max}} - A)$ are used again. In a computer program one can evaluate the position i of $|a_1, \ldots, a_N\rangle$ in the list of basis vectors according to

```
   Ak = A
   i = 1
   do k=N,2,-1
      do n=0,BasisVector(k)-1
         i = i + D(k-1,Ak-n+1)
      enddo
      Ak = Ak - BasisVector(k)
   enddo
```

`BasisVector` contains the N entries a_k. If the array of dimension $D(N, A)$ is properly initialized, i.e. the field value is zero for non-valid combinations of N and A, then the sum can be performed in a computer program without paying attention to the restrictions for the indices.

References

1. W. F. Giauque and D. MacDougall, Phys. Rev. **43**, 768 (1933).
2. M. Evangelisti *et al.*, Appl. Phys. Lett. **87**, 072504 (2005).
3. M. Manoli *et al.*, Angew. Chem. Int. Ed. **46**, 4456 (2007).
4. M. Evangelisti *et al.*, Phys. Rev. B **79**, 104414 (2009).
5. J. W. Sharples *et al.*, Chem. Commun. **47**, 7650 (2011).
6. Y.-Z. Zheng, M. Evangelisti, and R. E. P. Winpenny, Chem. Sci. **2**, 99 (2011).
7. T. N. Hooper *et al.*, Angew. Chem. Int. Ed. **51**, 4633 (2012).
8. R. Sessoli, Angew. Chem. Int. Ed. **51**, 43 (2012).
9. R. Schnalle and J. Schnack, Phys. Rev. B **79**, 104419 (2009).
10. R. Schnalle and J. Schnack, Int. Rev. Phys. Chem. **29**, 403 (2010).
11. J. Jaklic and P. Prelovsek, Phys. Rev. B **49**, 5065 (1994).

12. J. Jaklic and P. Prelovsek, Adv. Phys. **49**, 1 (2000).
13. J. Schnack and O. Wendland, Eur. Phys. J. B **78**, 535 (2010).
14. M. E. Zhitomirsky, Phys. Rev. B **67**, 104421 (2003).
15. J. Schnack, R. Schmidt, and J. Richter, Phys. Rev. B **76**, 054413 (2007).
16. A. Honecker and M. E. Zhitomirsky, J. Phys.: Conf. Ser. **145**, 012082 (4pp) (2009).
17. J. Schnack, Dalton Trans. **39**, 4677 (2010).
18. M.-J. Martinez-Perez *et al.*, Adv. Mater. (2012), in press.
19. M. Aichhorn, M. Daghofer, H. G. Evertz, and W. von der Linden, Phys. Rev. B **67**, 161103 (2003).
20. J. C. Plakatouras *et al.*, J. Chem. Soc., Chem. Commun. 2455 (1994).
21. B.-Q. Ma *et al.*, New J. Chem. **24**, 251 (2000).
22. B.-Q. Ma *et al.*, Angew. Chem. Int. Ed. **39**, 3644 (2000).
23. A. Rohde and W. Urland, Dalton Trans. 2974 (2006).
24. N. Kato *et al.*, J. Am. Chem. Soc. **128**, 6768 (2006).
25. X.-J. Kong *et al.*, Inorg. Chem. **48**, 3268 (2009).
26. J. Schnack, M. Luban, and R. Modler, Europhys. Lett. **56**, 863 (2001).
27. S. Sanz *et al.*, Chem. Commun. **48**, 1449 (2012).
28. J. Schnack, P. Hage, and H.-J. Schmidt, J. Comput. Phys. **227**, 4512 (2008).
29. K. Bärwinkel, H.-J. Schmidt, and J. Schnack, J. Magn. Magn. Mater. **212**, 240 (2000).
30. E. R. Gagliano, E. Dagotto, A. Moreo, and F. C. Alcaraz, Phys. Rev. B **34**, 1677 (1986).
31. H. Q. Lin, Phys. Rev. B **42**, 6561 (1990).